

Quasiparticle resonant states as a probe of short-range electronic structure and Andreév coherence

Michael E. Flatté

Department of Physics and Astronomy, University of Iowa, Iowa City, IA 52242

Abstract

The recently observed properties of quasiparticle resonant states near impurities on the surface of superconducting $\text{Bi}_2\text{Sr}_2\text{CaCu}_2\text{O}_{8+\delta}$ demonstrate that in-plane Andreév processes are either absent or phase-incoherent. Analysis of the spectral and spatial details of the electronic structure near a Zn impurity also suggest an effective magnetic component of the impurity potential. Further experiments are proposed to clarify whether the effective moments of nearby impurities are correlated.

Over the past few years several authors have emphasized the wealth of information available from local probes of impurity properties in correlated electron systems, and particularly in superconductors whose homogeneous order parameters (OP) are anisotropic in momentum [1]. A parallel improvement in scanning tunneling spectroscopy (STS) has allowed this vision to become a reality through direct observation of the local density of states (LDOS), first in niobium [2], which has a momentum-independent OP, and this year in the high-temperature superconductor $\text{Bi}_2\text{Sr}_2\text{CaCu}_2\text{O}_{8+\delta}$ (BSCCO) [3–5], which has an anisotropic OP. The electronic structure of the BSCCO surface is much more complex than that of the niobium surface; there are local moments in the copper-oxygen planes and, under certain conditions, a pseudogap state. Recent work [6] has emphasized the role of the pseudogap state [7–9] in determining the properties of clean surfaces of high-temperature superconductors at temperatures near T_c , and STS and photoemission have directly demonstrated its existence on the surface of BSCCO. The pseudogap state is characterized by a single-particle gap of $d_{x^2-y^2}$ symmetry, but the Andreev processes one would expect in a superconducting state are (according to differences in mechanism) either absent or phase-incoherent.

Here the STS measurements near impurities [3–5] will be shown to unambiguously demonstrate essentially complete suppression of Andreev processes in the vicinity of the impurity, even at very low temperatures. This low-temperature indication of a pseudogap implies its importance to the nature of the superconducting state and the operation of devices (such as Josephson junctions) with such materials. Indications of an effective magnetic component can also be seen in Ref. [5]. Thus STS provides a direct probe of both the local Andreev (superconducting) coherence and the local magnetic properties on the BSCCO surface.

A brief review of the experimental results from Refs. [3–5] is in order. Theoretical predictions which have been confirmed include the presence of quasiparticle resonances near nonmagnetic impurities in anisotropic OP superconductors [10], as well as the suppression of the gap feature near the impurity and the asymmetry of the resonance peak due to the energy dependence of the quasiparticle density of states [11]. The disagreements with previous theory, however, are striking. The most noticeable one is that the resonant state has only been detected on the *hole* side of the spectrum, both on the impurity site and *everywhere else around the impurity*. Whereas previous theories are consistent with an LDOS measured at the impurity which is entirely hole-like, these same theories unambiguously predict the LDOS at nearest-neighbor states will be almost entirely electron-like. Indeed these theories predict the spatially-integrated LDOS (or DOS) will be nearly particle-hole symmetric even though the LDOS at any particular site is not. A second unexpected element in the data is the presence of a second, much smaller, spectral peak on the hole side in Ref. [5]. Whereas previous theories are consistent with two resonances at a single impurity, the spatially-integrated amplitude of each resonance should be approximately the same, unlike what is seen in Ref. [5].

The above two issues are disagreements between the experimental and theoretical DOS, but there are also two significant disagreements in the LDOS. The resonance has a large amplitude at the impurity site, whereas calculations indicate that the largest amplitude in the LDOS should occur at the nearest-neighbor sites. Finally, the gap feature is seen on the impurity site, where it does not appear in calculations. [1]

The calculations here incorporate the pseudogap state into the evaluation of the dif-

ferential conductance (dI/dV). After evaluating the LDOS for several impurity potential models, allowing for spatial extent and magnetic character in the potential, the impurities of Refs [3–5] are found to be highly localized and the four discrepancies above can be reconciled. Finally, in the case of Ref. [5], a magnetic component to the effective Zn impurity potential is evident. [12]

The calculations of the LDOS are based on the Hamiltonian

$$H = \sum_{\langle ij \rangle, \sigma} \left[-t_{ij} c_{i\sigma}^\dagger c_{j\sigma} + \Delta_{ij} c_{i\uparrow}^\dagger c_{j\downarrow}^\dagger + \Delta_{ij}^* c_{j\downarrow} c_{i\uparrow} \right] + \sum_i \left[(V_{0i} + V_{Si}) c_{i\uparrow}^\dagger c_{i\uparrow} + (V_{0i} - V_{Si}) c_{i\downarrow}^\dagger c_{i\downarrow} \right], \quad (1)$$

which includes a site-dependent potential which can be magnetic (V_S), nonmagnetic (V_0), or a combination of both. i and j label sites and σ labels spin. The homogeneous electronic structure, expressed as hopping matrix elements (t_{ij}) for the first five nearest neighbors, is taken from a single-band parametrization of photoemission data. [13] Large variations in hopping matrix elements (> 50 meV) produce results very much at odds with experiment, whereas smaller variations are mimicked by the site-dependent potential. Hence such changes will be ignored here. Only on-site and nearest-neighbor order parameters Δ_{ij} are nonzero, and the maximum OP on the Fermi surface, $\Delta_{max} = 40$ meV. [14]

The electronic structure of the inhomogeneous system (including the impurity) is determined by direct numerical solution in real space of the Gor'kov equation (in Nambu form) for the inhomogeneous Green's function, $\mathbf{G} = \mathbf{g} + \mathbf{g}\mathbf{V}\mathbf{G} = (\mathbf{I} - \mathbf{g}\mathbf{V})^{-1}\mathbf{g}$, within a real-space region around the impurity beyond which the potential is negligible. [1] The Δ_{ij} 's are found self-consistently in this process, for they determine the off-diagonal components of the potential \mathbf{V} . Spectra outside this real-space region are constructed according to the generalized \mathbf{T} -matrix equation: $\mathbf{G} = \mathbf{g} + \mathbf{g}\mathbf{V}[\mathbf{I} - \mathbf{G}\mathbf{V}]^{-1}\mathbf{g}$. Once \mathbf{G} has been calculated throughout the region near the impurity, the LDOS and DOS are obtained from its imaginary part and the lattice Wannier functions. Then

$$\frac{dI(\mathbf{x}; V)}{dV} = - \int d\omega \sum_{\sigma} \frac{1}{\pi} \left(\frac{\partial n_{STM}(\omega)}{\partial \omega} \right) |\phi_{\sigma}(\mathbf{x}; i)|^2 \text{Im} G_{\sigma}(i, i; \omega), \quad (2)$$

where $\phi_{\sigma}(\mathbf{x}; i)$ is the overlap of the Wannier function at site i and spin σ with the STM tip at \mathbf{x} , and $n_{STM}(\omega)$ is the occupation function of the STM tip. [1] Resonances correspond to new peaks in the differential DOS (the difference between the inhomogeneous and homogeneous DOS); their energies are shown in Fig. 1(ab) for magnetic and nonmagnetic single-site impurities.

If Andreév processes are suppressed, either by reduction in their amplitude or phase coherence, a resonance's DOS will become more electron-like or more hole-like. Reduction of the amplitude of the homogeneous anomalous Green's function $f(i, j; \omega)$, due perhaps to a local antiferromagnetic (AF) order, decreases the mean-field coupling between electron and hole excitations. Note that this is very different from the fully electron or hole-like character of the LDOS at the impurity, which originates from a vanishing $f(i, i; \omega)$ in the $d_{x^2-y^2}$ state. Figure 1(cd) shows the DOS of a resonance for three systems with a 40 meV $d_{x^2-y^2}$ gap: a fully superconducting gap (solid line), a gap with a 25 meV superconducting component (dashed line), and a pseudogap with no superconducting component (dot-dashed line). As the superconducting component is reduced, the electron-hole symmetry diminishes. The nonmagnetic potentials of Fig. 1(c) are chosen (1.375 eV, 1.000 eV, and 0.833 eV,

respectively) so the resonance peak is at -1.5 mV (the same as Ref. [5]). The magnetic potentials in Fig. 1(d) are the same as those in Fig. 1(c).

The reduction of the electron-like peak from phase decoherence is similar to the effect of amplitude suppression of $f(i, i; \omega)$. For a resonance at ω , the peak at $-\omega$ comes from terms with products of pairs of anomalous Green's functions. For a phase incoherent pseudogap state the expectation value of these pairs, and thus the amplitude of the electron-like peak, is diminished. [8] The effect of this is shown in Fig. 1(e,f) as a dashed line corresponding to partial (half) and a dot-dashed line corresponding to no phase coherence. The nonmagnetic potential is 1.375 eV in Fig. 1(e) and the magnetic potential is 1.375 eV in Fig. 1(f). Note that for the purely magnetic impurities even in the absence of Andreév coherence there is a peak on each side of zero energy.

For Refs. [3,5] there is no apparent electron-like component of the resonance in the DOS, thus local Andreév coherence is absent. In measurements of the LDOS near metal islands on BSCCO [4], however, both hole-like and electron-like peaks are apparent. This may indicate that the metal plays an important role in maintaining phase coherence at the surface, or that the metal overlayer is less disruptive to superconductivity than impurities in the plane. The presence of the in-plane Andreév processes, indicated by the electron-like peak, is essential to the operation of Josephson junctions.

The on-site LDOS of Ref. [5] is shown in Fig. 2(a). The second (hole-like) peak is not as clearly evident in the results of Refs. [3,4], and thus may be peculiar either to the Zn impurity or to the impurity site in the BSCCO unit cell. Additional resonances around impurities can originate from additional orbital states around spatially-extended potentials or from spin-splitting near magnetic potentials. Note that an effective magnetic potential could also originate from a nonmagnetic impurity potential placed in a spin-polarized host electronic structure.

Figure 2(abc) shows the best fit of dI/dV to the data of Ref. [5] for phase incoherent Andreév processes and i a single-site nonmagnetic potential (1.375 eV), ii a nonmagnetic potential with onsite (0.360 eV) and nearest-neighbor (0.150 eV) values, and iii a mixed nonmagnetic and magnetic potential ($V_0 = 0.825$ eV, $V_S = 0.550$ eV). Also shown is the best fit using iv a pseudogap with no superconducting component and a mixed potential ($V_0 = 0.543$ eV, $V_S = 0.290$ eV). The three panels show dI/dV (a) at the impurity site, (b) at the nearest-neighbor site along the gap nodes, and (c) along the gap maxima. Measurements of Ref. [5] for (a) and (b) are shown; (c) is not available.

The large size of the resonance on-site and the simultaneous presence of the gap feature occur because of junction normalization (equal resistance at -200 mV) and the finite width of the $|\phi_\sigma|^2$ (modeled as Gaussians of range 0.8\AA , 3.8\AA , 0.8\AA , and 1.0\AA for i - iv). The very small LDOS in this energy range at the impurity site causes the tip to approach closer to the surface and (1) enlarge the apparent size of the resonance on-site, and (2) pick up the gap features from the nearest-neighbor sites. The relative size of the on-site resonance to the gap features is largely determined by the overlap of the nearest-neighbor Wannier functions with the tip when the tip is over the impurity site.

Judging from the comparison with experiment, iii and iv appear most in agreement. i does not have a second resonance, and whereas ii does show one in the proper location, its relative magnitude is incorrect. The smaller amplitude of the second resonance is obtained for iii and iv because the overlaps with the STM tip are spin-dependent ($|\phi_\uparrow(\mathbf{x})|^2/|\phi_\downarrow(\mathbf{x})|^2 \sim$

40). If the second peak were absent, either the impurity would lack magnetic character, or it would occur in less magnetic regions of the BSCCO unit cell. The remaining disagreement is in the amplitude of the resonance in (B), where *iv* is best, but still too small.

Figure 3 shows the amplitude of the resonance as a function of distance from the impurity along the gap maxima (a) and the gap nodes (b). The squares are the data from Ref. [5], whereas the solid line corresponds to *iii*, the dotted line to *ii*, and the dot-dashed line to *iv*. The plot for *i* looks identical to that of *iii*. The agreement of *iii* and *iv* are quite good along the maxima direction. The absence of a well-defined maximum at the nearest-neighbor in (a), which was pointed out in Ref. [5], is due to the normalization procedure. An inset in Fig. 3 shows the difference between the junction normalized (solid) and unnormalized (dashed) dI/dV . The main discrepancy is with the amplitude of the signal along the node directions (b).

Figure 4 shows the dI/dV of the resonance for *iv*; *iii* is similar. The differences between the Figs. 2-4 and the measurements of Ref. [5] may be due to errors in the homogeneous electronic structure of BSCCO used in the calculation, particularly the low-energy electronic structure which dominates the longer-range LDOS. These errors may be due to inaccuracies in the model for the electronic structure measured by photoemission [13], or they may be due to the neglect of other collective effects on the surface. Another likely source of error is that the electronic structure model of the host is not spin dependent.

One of the possible mechanisms of a pseudogap is local AF order, such as occurs in a stripe. [9] The magnetic component apparent in the impurity potential suggests this origin as well. If two nearby local moments are aligned parallel, then the resonances associated with them will hybridize and split [15], whereas if they are antiparallel the resonances will be degenerate. A careful examination of the dI/dV for two Zn atoms near each other on the surface may clarify whether there is local AF order.

The LDOS reported in Refs. [3–5] are best explained by the presence of a pseudogap state on the surface of BSCCO. The relative height of the electron-like and hole-like resonances in the DOS depends directly on the amplitude of local Andreev processes, and thus shows the degree of local superconducting coherence. This is of great practical interest, for the presence of these processes is essential to forming a proper Josephson junction across an interface. The information obtained about the superconducting state at the surface of BSCCO indicates the clear promise of future STM measurements near defects in other correlated electron systems.

I would like to thank J. C. Davis for discussions and for providing the data of Ref. [5]. This work has been supported in part by ONR through contract No. N00014-99-1-0313.

REFERENCES

- [1] See M. E. Flatté and J. M. Byers, in *Solid State Physics Vol. 52*, ed. H. Ehrenreich and F. Spaepen, (Academic Press, New York, 1999), and references therein.
- [2] A. Yazdani, *et al.*, *Science* **275**, 1767 (1997).
- [3] E. W. Hudson, *et al.*, *Science* **285**, 88 (1999).
- [4] A. Yazdani *et al.*, *Phys. Rev. Lett.* **83**, 176 (1999).
- [5] S. H. Pan, *et al.*, *Nature (London)* in press (cond-mat/9909365).
- [6] A. G. Loeser, *et al.*, *Science* **273**, 325 (1996); Ch. Renner, *et al.*, *Phys. Rev. Lett.* **80**, 149 (1998).
- [7] G. V. M. Williams, *et al.*, *Phys. Rev. Lett.* **78**, 721 (1997); G. Deutscher, *Nature (London)* **397**, 410 (1999).
- [8] L. B. Ioffe and A. J. Millis, *Science* **285**, 1241 (1999).
- [9] V. J. Emery and S. A. Kivelson, *Nature (London)* **374**, 434 (1995).
- [10] M. A. Salkola, A. V. Balatsky, and D. J. Scalapino, *Phys. Rev. Lett.* **77**, 1841 (1996).
- [11] M. E. Flatté and J. M. Byers, *Phys. Rev. Lett.* **80**, 4546 (1998).
- [12] This has been seen in YBCO (A. V. Mahajan, *et al.*, *Phys. Rev. Lett.* **72**, 3100 (1994)).
- [13] M. R. Norman, M. Randeria, H. Ding, and J. C. Campuzano, *Phys. Rev. B* **52**, 615 (1995).
- [14] Measured gap features at the surface vary from sample to sample as well as from point to point on the same sample. 40 meV is a typical location for the gap feature.
- [15] M. E. Flatté and D. E. Reynolds, to be published (cond-mat/9912195).

FIGURES

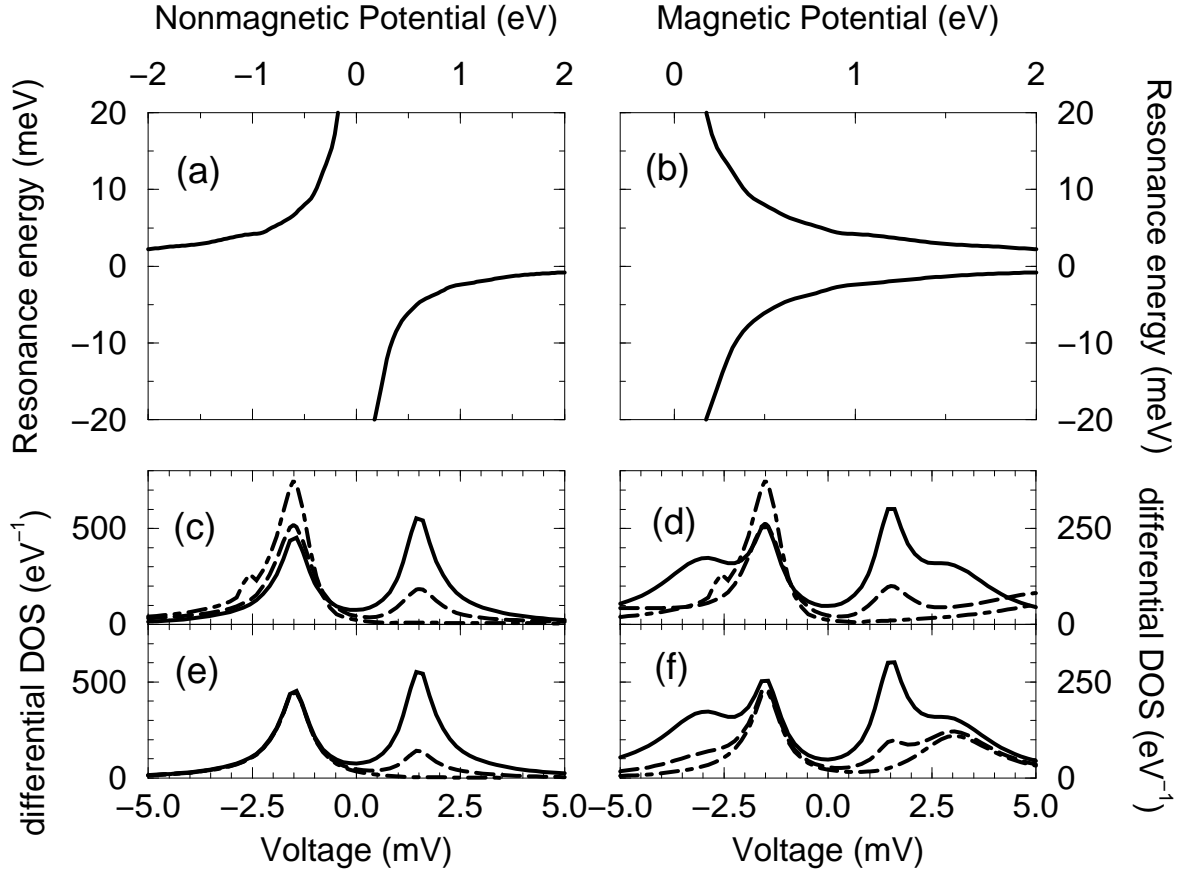


FIG. 1. Resonance energies for single-site (a) nonmagnetic and (b) magnetic impurity potentials. DOS for (c) nonmagnetic and (d) magnetic impurity potentials which produce a resonance at -1.5mV . Solid, 40 meV superconducting gap, dashed, 25 meV superconducting, 40 meV total gap, dot-dashed, 40 meV non-superconducting gap. (e) and (f), same as (c) and (d) except the dashed line corresponds to partial and the dot-dashed line to no phase coherence in the 40 meV superconducting system.

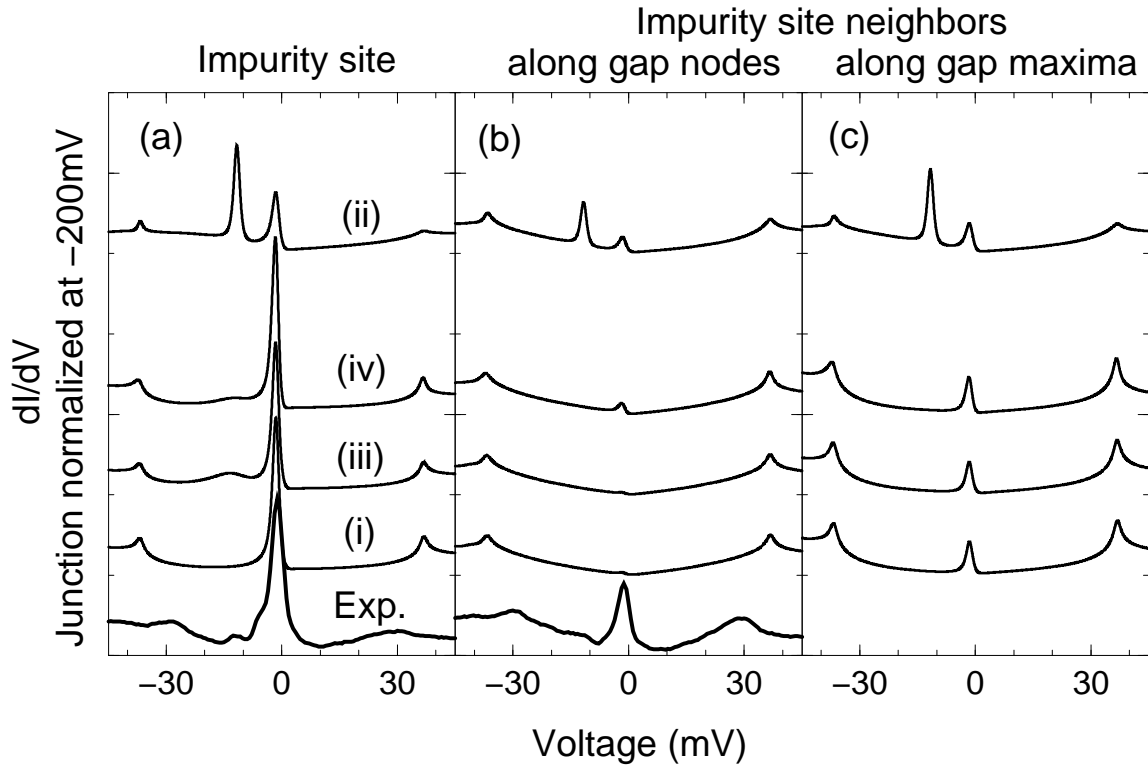


FIG. 2. dI/dV (a) on-site, (b) at the nearest-neighbor along the gap nodes, and (c) along the gap maxima, for impurity and host models i , ii , iii , and iv . Data of Ref. [5] is also shown. The order of vertical offsets (introduced for clarity) of the curves in (b) and (c) is the same as in (a).

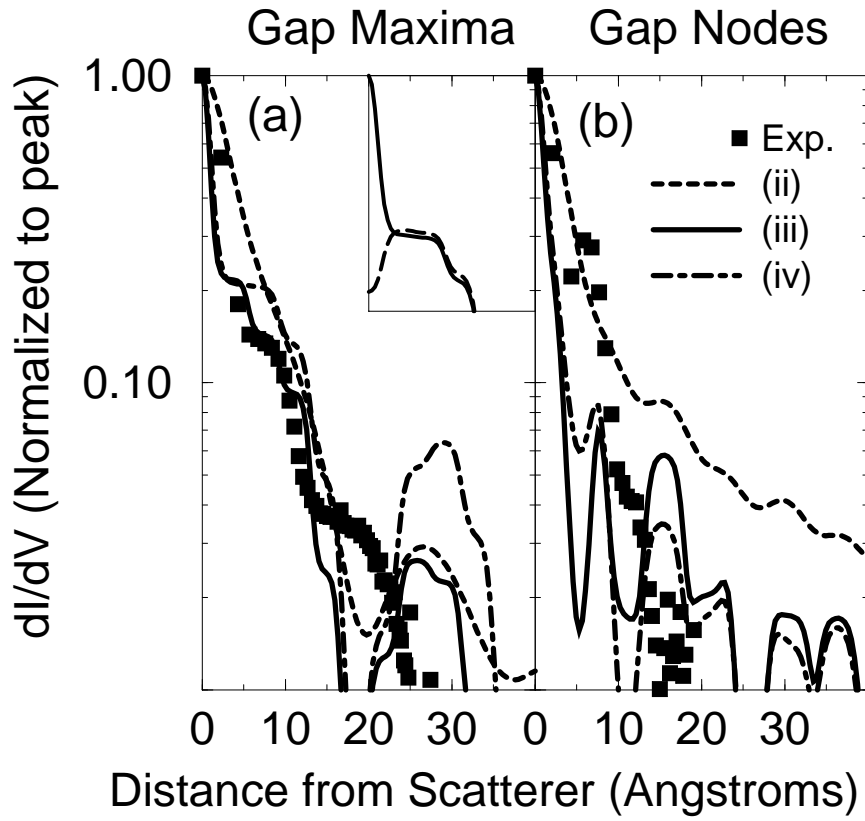


FIG. 3. dI/dV as a function of position along (a) the gap maxima and (b) the gap nodes. *ii* is dotted, *iii* is solid, and *iv* is dot-dashed. Shown in inset is the difference between dI/dV when junction normalization is (solid) and is not (dashed) taken into account.

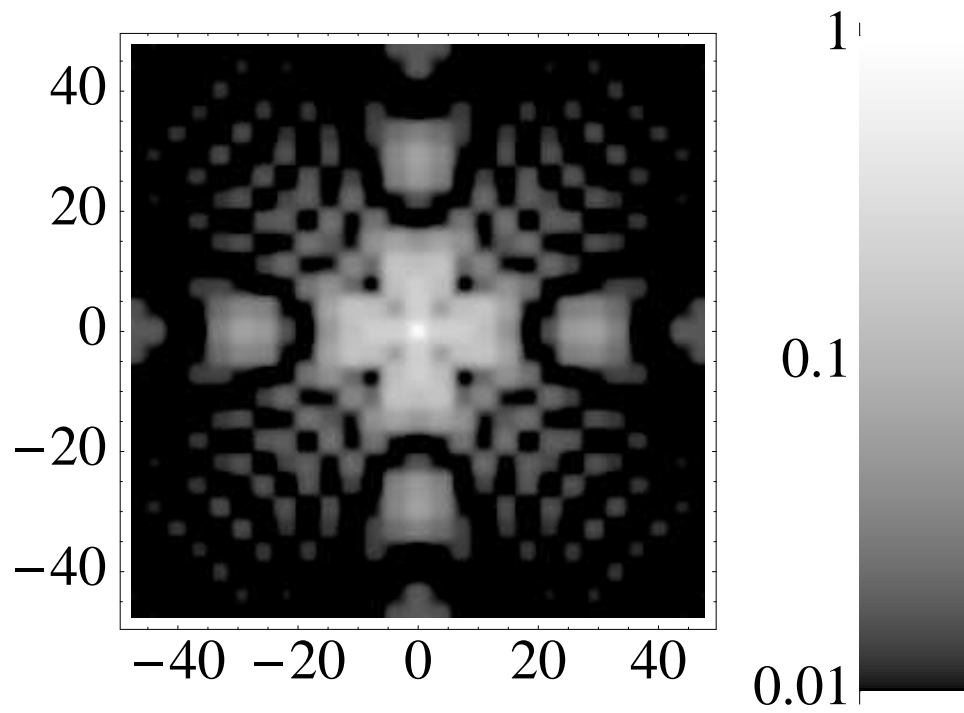


FIG. 4. Spatial structure of the dI/dV at the impurity resonance voltage (-1.5 mV) for iv . Horizontal is parallel to the gap maxima directions.